Swimming in needlefish (Belonidae): anguilliform locomotion with fins

James C. Liao

Department of Organismic and Evolutionary Biology, Harvard University, Cambridge, MA 02138 USA

e-mail: jliao@oeb.harvard.edu

Summary

The Atlantic needlefish (*Strongylura marina*) is a unique anguilliform swimmer in that it possesses prominent fins, lives in coastal surface-waters, and can propel itself across the surface of the water to escape predators. In a laboratory flow tank, steadily swimming needlefish perform a speed-dependent suite of behaviors while maintaining at least a half wavelength of undulation on the body at all times. To investigate the effects of discrete fins on anguilliform swimming, I used high-speed video to record body and fin kinematics at swimming speeds ranging from 0.25 to $2.0\,L\,\mathrm{s}^{-1}$ (where L is the total body length). Analysis of axial kinematics indicates that needlefish are less efficient anguilliform swimmers than eels, indicated by their lower slip values. Body amplitudes increase with swimming speed, but unlike most fishes, tail-beat amplitude increases linearly and does not plateau at maximal swimming speeds. At $2.0\,L\,\mathrm{s}^{-1}$, the propulsive wave shortens and decelerates as it travels posteriorly, owing to the prominence of the median fins in the caudal region of the body. Analyses of fin kinematics show that at $1.0\,L\,\mathrm{s}^{-1}$ the dorsal and anal fins are slightly less than 180° out of phase with the body and approximately 225° out of phase with the caudal fin. Needlefish exhibit two gait transitions using their pectoral fins. At $0.25\,L\,\mathrm{s}^{-1}$, the pectoral fins oscillate but do not produce thrust, at $1.0\,L\,\mathrm{s}^{-1}$ they are held abducted from the body, forming a positive dihedral that may reduce rolling moments, and above $2.0\,L\,\mathrm{s}^{-1}$ they remain completely adducted.

Key words: needlefish, *Strongylura marina*, anguilliform locomotion, steady swimming, pectoral fin kinematics, positive dihedral, median fin, acceleration specialist.

Introduction

Anguilliform locomotion is widespread among aquatic animals and represents a convergent strategy for moving through water. Since Gray's pioneering work on a swimming juvenile *Anguilla vulgaris* (now *Anguilla anguilla*) (Gray, 1933), comprehensive and comparative analyses of anguilliform swimmers have revealed substantial variability in swimming kinematics. Although sources of this variability may include differences in neuromuscular control, ontogeny, swimming speed and phylogenetic history, a substantial component of the variation in kinematics may be due '*to the external morphological differences in the shape of the trunk and the tail*' (Gillis, 1996). Thus, a promising approach to understanding the causal basis for differences in anguilliform swimming kinematics is to make use of the morphological diversity found among anguilliform swimmers.

Elongate fishes in several phylogenetically and ecologically disparate families exhibit undulatory locomotion. In addition to the catadromous eels (Anguillidae), examples range from jawless fishes such as stream-dwelling lampreys (Petromyzontidae), to highly derived Perciformes such as rocky intertidal gunnels (Pholidae) and burrowing sand lances (Ammodytidae) (Nelson, 1994). In general, elongate fishes that swim using undulatory locomotion tend to live in benthic, structurally complex environments, are slow-to-moderate swimmers, and often have reduced or lost fins (Helfman et al., 1997).

An exception is the Atlantic needlefish (*Strongylura marina*), an elongate teleost related to the flying fishes (Exocoetidae) that lives in the surface waters of coastal marine environments. The behavior of *S. marina* leaping and skittering across the surface at high speeds when alarmed is well known (Collette, 1977; Helfman et al., 1997) and has prevented them from being studied in captivity. Breder (1926) observed them more than 70 years ago, but thought them to be '*rigid fishes…resembling esocids*' whose swimming movements were not as close to the '*anguilliform type of motion as might be expected judging from the form alone*'. Needlefish possess a posterior arrangement of distinct, dorsal, anal and caudal fins that is unusual for anguilliform swimmers. Unlike in most elongate undulatory fishes, the bases of their relatively large pectoral fins are oriented closer to vertical than to horizontal (Collette, 1977; Helfman et al., 1997). No kinematic studies to date have described the axial kinematics of anguilliform locomotion in acanthopterygian fishes. In addition, there are no data on the fin kinematics of anguilliform swimming fishes, despite the

fact that the median fins may contribute substantially to the lateral body profile.

Kinematic analyses of anguilliform swimmers have not emphasized the contribution of the fins since the principal force component is assumed to be generated predominantly by the body axis (Gillis, 1998). However, experimental work on several genera of fishes has shown that fins can alter the flow associated with the body as well as with other fins (Webb and Keyes, 1981; Jayne et al., 1996; Wolfgang et al., 1999; Nauen and Lauder, 2000; Hove et al., 2001). As we approach a more comprehensive understanding of fish locomotion, it is clear that kinematic analyses integrating both the body and fin movements are needed.

In this study, I examine the body and fin kinematics of steadily swimming needlefish and suggest some hydrodynamic consequences of having fins on an elongate body. The specific goals of this paper are (i) to describe the axial body kinematics of the Atlantic needlefish and highlight how they differ from other anguilliform swimmers, and (ii) to document the change in pectoral and median fin kinematics across speeds and discuss their possible functional roles.

Materials and methods

Animals

Adult Atlantic needlefish, *Strongylura marina* Walbaum, were obtained from the New England Aquarium in Boston, MA, USA. Fish were housed in a 1200 l circular polyvinyl chloride tank maintained at a temperature of $24\pm1°C$ and a salinity of 32–34‰. Fish were fed dried euphausiids, frozen silversides (*Menidia* spp.) and brine shrimp (*Artemia* sp.). Data were collected from four individuals (total body length, $L=23.3\pm1.5$ cm, mean $\pm$ S.E.M.).

Experimental procedures

Fish were acclimated to the flow tank for several hours before data were collected. Experiments were conducted in a 600 l aerated, recirculating flow tank (working section 28 cm$\times28$ cm$\times80$ cm) maintained at $24\pm1°C$. Two electronically synchronized NAC HSV-500 video cameras filming at 250 frames s^{-1} simultaneously recorded ventral and posterior views of swimming needlefish using two 45° front-surface mirrors placed below the flow tank and within the flow tank, respectively.

Up to five swimming speeds were chosen because they encompassed the widest range of speeds over which needlefish would swim steadily in the flow tank (0.25, 0.5, 1.0, 1.5 and $2.0 L$ s^{-1}). These speeds were selected because needlefish can swim steadily at each for at least 30 min without exhibiting burst-and-coast behavior. To ensure that swimming speed was equivalent to flow velocity, data were collected only for fish swimming steadily in the center of the flow tank at least 12 cm away from the side walls. Swimming speeds

were tested in no particular order; however, needlefish could only swim steadily at high speeds if flow velocity was increased gradually. For most analyses, the four tail-beat cycles recorded for each fish at each swimming speed were consecutive.

Body analysis of anguilliform locomotion

For each tail-beat trial, at least 20 video frames were captured, separated in time by 12–20 ms, depending on the swimming speed of the fish. A customized software program was used to digitize 20 points on each side of the outline of the ventral silhouette of the fish (Fig. 1), for a total of 40 points for each image (note that the point placed on the tip of the jaw for left and right side overlap). A series of cubic spline functions were used to draw the best-fit line along these points (Jayne and Lauder, 1995; Gillis, 1997), and a midline was constructed and divided into 25 segments. The amplitudes relative to the midline for seven approximately equidistant points along the midline (Fig. 1) were calculated by dividing the total lateral excursion during one oscillatory cycle by two. The first location (Fig. 1, 0% L) coincided with the tip of the
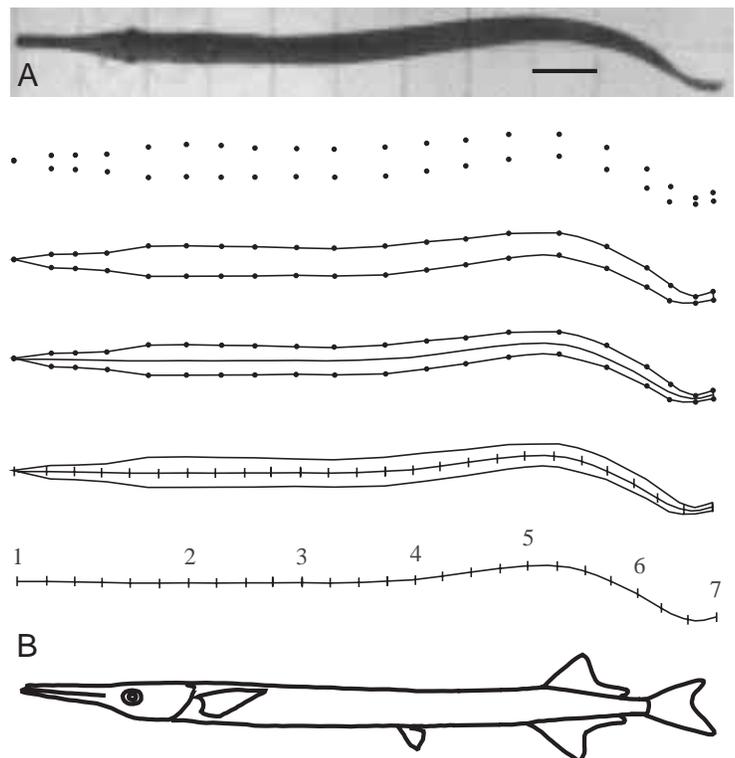

Fig. 1. (A) Ventral view of a needlefish swimming at $1.0 L$ s^{-1} (where L is the total body length), with subsequent digitized outlines (below) based on 40 digitized points and midline reconstructions from a customized spline-fitting program. Scale bar, 2 cm. (B) Lateral tracing of a needlefish. Point 1 corresponds to the tip of the jaw, point 2 corresponds to the edge of the operculum, and point 7 corresponds to the tip of the ventral lobe of the tail. Note that a point 80% down the body corresponds to the tip of the dorsal and anal fins.

dentary, the second location (24% *L*) marked the body just posterior to the operculum, the third through to sixth locations (40–88% *L*) divided the body of the fish, and the seventh location (100% *L*) represented the tip of the tail. To characterize body amplitudes during gait transitions over the broadest range of swimming speeds, analysis of the seven body amplitudes focused on three speeds, including the lowest and highest speeds (0.25, 1.0 and 2.0 $L\,s^{-1}$, *N*=16 wave cycles for each speed).

All five steady swimming speeds were analyzed to better examine the relationship between swimming speed and tail-beat frequency. Mean tail-beat frequencies for each speed were determined for each fish (Fig. 3, *N*=4). This was accomplished by tracking a digitized point on the tail from the ventral view over the course of one tail-beat cycle and dividing it by the elapsed time. The time required to complete one tail-beat cycle is the tail-beat period. Stride length is the distance traveled per tail beat, calculated by dividing the swimming speed by the tail-beat frequency.

Consistent with Gillis (1998), propulsive wavelength was measured directly from the reconstructed midlines as the distance between two successive peaks present on the body. Although wavelength can be calculated by dividing the mean wave speed by the mean tail-beat frequency (Webb et al., 1984), this method consistently underestimated the propulsive wavelength compared to direct measurements from the midline. Furthermore, this method assumes a constant wave speed along the body, which prohibits analysis on fast-swimming needlefish.

Mean propulsive wave speeds for three swimming speeds, (0.25, 1.0 and 2.0 $L\,s^{-1}$) were calculated for all fish. Wave speed was calculated by dividing the distance between the anteriormost point of the body exhibiting undulation and the tail tip by the time required for the crest of the wave to pass through these points. At high speeds, a larger portion of the body undulates, allowing the crest of the propulsive wave to be tracked from a more anterior position than would be possible at lower swimming speeds. Slip was calculated as *U*/*V* and Froude efficiency as 1–0.5[(*V*–*U*)/*V*] (Lighthill, 1975), where *U* is the swimming speed and *V* is the propulsive wave speed.

To determine the possible effect of the median fins on the speed of the propulsive wave along the body, changes in wave speed were investigated for the two extreme swimming speeds. Differences in the propulsive wave speed were determined by halving the entire region of the body that was undulating and calculating the speed for each section. Thus, the anterior section of the propulsive wave (72–84% *L*) at 0.25 $L\,s^{-1}$ was different from the anterior section of the propulsive wave (24–60% *L*) at 2.0 $L\,s^{-1}$ (Fig. 1). Since undulation is restricted to the back of the body at 0.25 $L\,s^{-1}$, the anterior and posterior halves of the undulating region contain a similar portion of the median fins. In contrast, because a larger portion of the body undulates at 2.0 $L\,s^{-1}$, the anterior half of the propulsive wave is void of the median fins, which are now completely contained within the posterior half.

Analysis of fin kinematics

Needlefish fins are too delicate to be marked. However, images from the posterior view provided enough contrast to allow the apex of the dorsal and anal fins and the edge of the caudal and pectoral fins to be identified. To describe the phase relationships between the body and median fins, I analyzed four cycles for all fish swimming at 1.0 $L\,s^{-1}$, an intermediate speed at which needlefish swim steadily for the longest period of time. The longitudinal position of the dorsal and anal fin apices coincides with a point 80% down the body (Fig. 1), as measured on anesthetized individuals. Only a limited number of points that could be reliably identified using the outline of the fins were digitized. To perform a statistical analysis on median fin excursions, individual tail beats for all fish were aligned. Although this procedure resulted in depressed values for median fin amplitude compared to averaging maximum values (e.g. compare the tail-beat amplitude in Fig. 5 to that in Fig. 2), it accurately illustrates the average phasing of the fins relative to the body. Adduction and abduction speeds (mean of four trials for each of the four fish swimming at 0.25 $L\,s^{-1}$) for the pectoral fin were obtained by tracking the digitized tip of the fin. I measured the orientation and angle of insertion of the abducted pectoral fins using video images from the posterior view and lateral images of cleared and stained specimens, respectively. In addition, outline tracings of the fins at selected phases of adduction and abduction were produced by digitizing points around the edge of the fins using CorelDraw version 9.0 for the PC. The same technique was used to reconstruct the trailing edge of the caudal fin.

Statistical tests

Means and standard errors (S.E.M.) were calculated for the amplitudes at each of the seven body locations, tail-beat frequencies and the propulsive wave speeds for the anterior and posterior regions of the body across swimming speeds. A two-sample *t*-test was used to determine if there were differences in the mean speed of the pectoral fin tips during abduction and adduction in the *x* and *z* directions. A paired-sample *t*-test was performed to detect significant differences in the anterior and posterior propulsive wave speeds for needlefish swimming at 0.25 and 2.0 $L\,s^{-1}$. Two-way, mixed-model analyses of variance (ANOVA) were performed separately for tail-beat frequency, period and stride. Significance levels were adjusted using the sequential Bonferroni technique (Rice, 1989).

To examine the effect of individual, swimming speed and longitudinal position on body wave amplitude, a three-way mixed-model (Model III) ANOVA was used. Swimming speed and longitudinal position were treated as the fixed effects and the individual was considered to be the random effect. A Bonferroni–Dunn *post-hoc* test was performed to determine whether there were significant differences among swimming speeds and longitudinal position (α=0.05). *F*-values for all ANOVAs were calculated according to Zar (1999). Statistical tests were performed by Statview (version 4.5) for the PC.

Results

Body kinematics

Needlefish generate thrust by passing waves down their body at all swimming speeds. The amplitude of these waves increases from anterior to posterior (Fig. 2), and the percentage of the body that undulates increases with swimming speed. At $0.25\,L\,s^{-1}$, only the posterior 44% of the body undulates (including body point 4). At $1.0\,L\,s^{-1}$, all of the body posterior to the base of the cranium undulates (76% L). At $2.0\,L\,s^{-1}$, the amplitude of undulation increases along the body and the elongate cranium exhibits yawing motions (0.3% L). Above $2.0\,L\,s^{-1}$, needlefish switch to burst-and-coast swimming. Propulsive wavelength increases from 49–73% L over the range of swimming speeds tested.

Over the range of swimming speeds investigated, tail-beat amplitude increases and does not plateau (Fig. 2). At $0.25\,L\,s^{-1}$, tail-beat amplitude is 2.6% L, at $1.0\,L\,s^{-1}$, tail-beat amplitude is 3.9% L, and at $2.0\,L\,s^{-1}$, tail-beat amplitude is 6.3% L. The relationship between tail-beat amplitude and swimming speed is best approximated by the equation $a=0.49U_l + 0.46$ ($r^2=0.89$, $P<0.0001$), where a is length-specific tail-beat amplitude and U_l is length-specific swimming speed ($L\,s^{-1}$).

Tail-beat frequency also increases as a function of swimming speed, from $2.6\pm0.1\,Hz$ at $0.25\,L\,s^{-1}$ to $5.1\pm0.3\,Hz$ at $2.0\,L\,s^{-1}$ (mean ± S.E.M., $N=16$ cycles). This relationship is best described by the equation $f=1.5U_l+2.4$ ($r^2=0.98$, $P<0.0001$), where f is tail-beat frequency (Fig. 3A; Table 1). There is a significant difference in tail-beat frequency among individuals ($P<0.001$). Stride length increases with swimming speed (Fig. 3B). The effects of individual, swimming speed,

and the interaction between individual and swimming speed on tail-beat period and stride are significant to at least $P<0.01$ (Table 1).

Absolute body wave speed (Fig. 4A) increases with swimming speed according to the equation $V=30.9U_l+18$ ($r^2=0.88$, $P<0.0001$, $N=48$), where the regression is performed on the raw values for the three swimming speeds. Means are $25.8\pm0.3\,cm\,s^{-1}$, $48.8\pm2.1\,cm\,s^{-1}$ and $77.7\pm5.4\,cm\,s^{-1}$, for fish swimming at $0.25\,L\,s^{-1}$, $1.0\,L\,s^{-1}$ and $2.0\,L\,s^{-1}$, respectively (mean ± S.E.M., $N=16$ wave cycles).

At $0.25\,L\,s^{-1}$, the propulsive wave speed does not change significantly along the portion of the body that undulates ($\alpha=0.05$; Fig. 4B). However, at $2.0\,L\,s^{-1}$ (Fig. 4C), the propulsive wave speed of the anterior body section (light gray column) is higher than that of the posterior section (dark gray column, $P<0.001$), indicating that at the highest swimming speed the propulsive wave decelerates as it travels towards the tail. Estimated mechanical efficiency increases with swimming
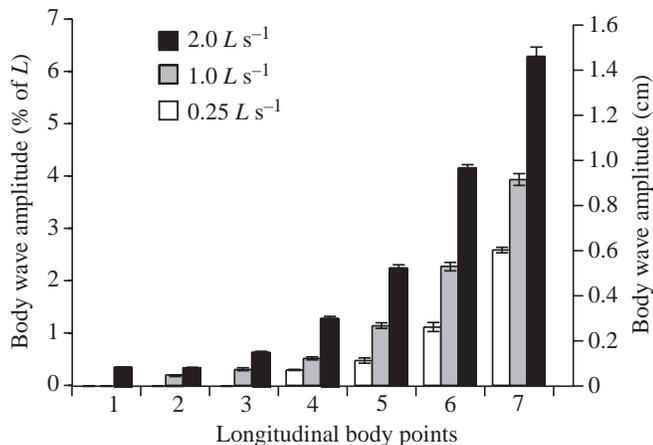
Fig. 3. (A) Tail-beat frequency (f) increases linearly with length-specific swimming speed (U_l). The equation for the line is $f=1.5U_l+2.4$ ($r^2=0.98$, $P<0.0001$). The regression is fitted to the mean tail-beat frequency values. (B) Stride length (distance moved for each tail beat) increases as swimming speed increases. Stride values are reported as a proportion of the total body length (L) as well as in absolute distance (cm). Values at each speed represent the mean of four tail beats (± S.E.M.) for each of the four individuals.

Fig. 2. Mean wave amplitudes (± S.E.M.) for seven points along the body for four fish at three swimming speeds. The y axes show amplitude as a percentage of the total body length (L) and in cm. Black bars, $2.0\,L\,s^{-1}$ (absolute speed $46.5\,cm\,s^{-1}$), gray bars, $1.0\,L\,s^{-1}$ (absolute speed $23.3\,cm\,s^{-1}$) and white bars, $0.25\,L\,s^{-1}$ (absolute speed $5.8\,cm\,s^{-1}$). At the lowest speed, only the posterior 44% of the body undulates. As the swimming speed increases, a larger proportion of the body undulates and the body wave amplitude increases non-linearly. Note that over the speeds tested the tail-beat amplitude (determined by tracking point 7) does not plateau.
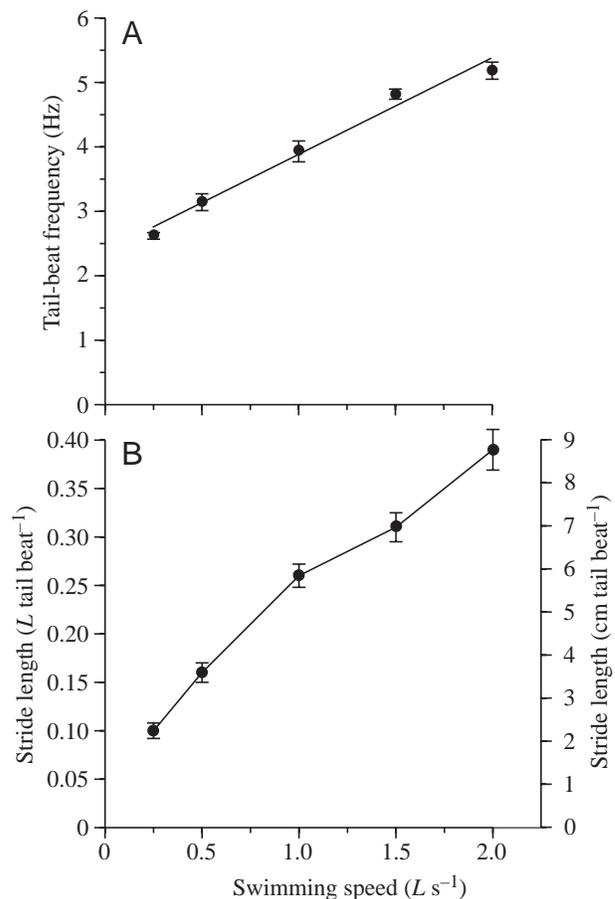
speed, as reflected in the slip values, which increase from 0.23±0.01 at 0.25 L s^{-1}, to 0.48±0.01 at 1.0 L s^{-1} and to 0.62±0.02 at 2.0 L s^{-1} (N=16 wave cycles). Froude efficiency also increases with speed, from 0.61 at 0.25 L s^{-1}, to 0.74 at 1.0 L s^{-1} and to 0.80 at 2.0 L s^{-1}.

Results from a three-way ANOVA (Table 2) treating longitudinal position, swimming speed and individual as effects and body-wave amplitude as the dependent variable show that amplitudes vary significantly with longitudinal positions, swimming speeds and individuals (P<0.001). Bonferroni–Dunn *post-hoc* tests indicate that the largest of the four fish (26 cm) has a significantly greater absolute body-wave amplitude than the other three fish (P<0.001). *Post-hoc* tests also reveal that the amplitudes corresponding to the yaw of the cranium did not change significantly with speed (P<0.001).

Fin morphology and kinematics

The dorsal and anal fins of needlefish taper abruptly from the anteriormost rays towards the tail, to form higher-aspect-ratio fins than otherwise found in anguilliform swimming fishes (Fig. 1B). Their combined surface area is greater than 116% of the caudal fin area, representing one of the most significant surfaces of the body interacting with water. Fully erect, the dorsal and anal fins provide a lateral profile that is three times the depth of the anterior region of the body. A phase relationship of slightly less than 180° between the anterior median fins and the body at the same longitudinal position (80% L) is maintained at a swimming speed of 1.0 L s^{-1} (Fig. 5). The lateral excursion of the dorsal and anal fins is approximately 1.7% L, similar to the lateral excursion of the body at 80% L. While the tips of the caudal fin show similar amplitudes to each other at 1.0 L s^{-1}, this is not true for the entire trailing edge, which adopts a complex dihedral conformation (Fig. 6).

At 0.25 L s^{-1}, the pectoral fins oscillate at a frequency of 3.41±0.46 Hz (mean ± S.E.M, N=16). Mean abduction speed (3.8±1.4 cm s^{-1}) along the x direction (Fig. 7) relative to the body is less than the mean adduction speed (4.7±1.1 cm s^{-1}, P=0.01), where the x direction corresponds to the path of the downstream flow. During adduction, the fins are oriented along the transverse plane (y, z), where the y direction corresponds to the vertical axis with respect to the flow tank and the z direction indicates the direction across the flow tank. Because the adduction speed in the x direction relative to the body is less than the forward swimming speed (5.8 cm s^{-1}), the pectoral fins do not generate thrust. Along the z direction, abduction speed

Table 1. *Summary of F-tests for significance of effects in three separate two-way ANOVAs for tailbeat frequency, period and stride length*

Variable	Individual	Speed	Speed× individual
Tail-beat frequency (Hz)	15.79* (3, 36)	46.38* (2, 6)	5.02** (6, 36)
Tail-beat period (ms)	16.84* (3, 36)	77.44* (2, 6)	3.948*** (6, 36)
Stride length (L)	26.18* (3, 36)	136.04* (2, 6)	7.523* (6, 36)

Data are from four individuals, four cycles per individual, at three swimming speeds.

Bonferroni-corrected two-way ANOVA (Rice, 1989); entries are *F*-values, degrees of freedom are in parentheses.

Significant at *P=0.001, **P=0.005, ***P=0.01.

is 6.3±1.2 cm s^{-1} and adduction speed is 8.4±1.4 cm s^{-1} (mean ± S.E.M., N=16). As intermediate swimming speeds are approached, needlefish switch to holding their pectoral fins out as a positive dihedral (Fig. 8B), while at high speeds they fold
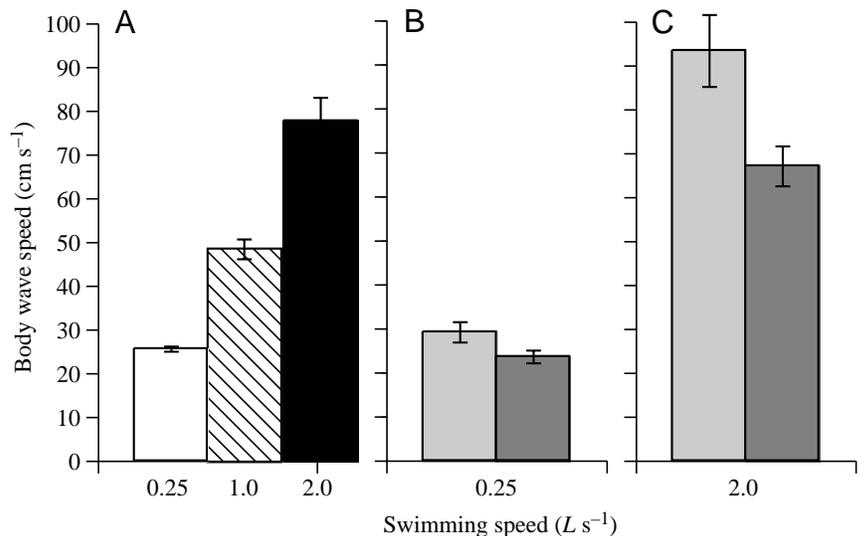

Fig. 4. (A) Mean propulsive wave speed for the lowest (white), middle (hatched), and highest (black) swimming speeds (mean ± S.E.M., N=16 cycles). Wave speed was determined by calculating the time required for a wave to travel past two points of a known distance. Note that the proportion of the body that undulates depends on the swimming speed. In each case, the body wave traveled posteriorly faster than the forward speed of the fish. (B) Changes in propulsive wave speed down the body were investigated for the two extreme swimming speeds. At 0.25 L s^{-1}, only a small region of the body undulates. When that region is divided in half, both the anterior (light gray column) and posterior (dark gray column) section contain part of the dorsal and anal fins. Wave speeds for the two segments are not significantly different (α=0.05). (C) At 2.0 L s^{-1}, the entire body undulates except for the rigid neurocranium. Due to the presence of the median fins, the posterior section of the propulsive wave is significantly slower (P<0.001) than the anterior section, reflecting an overall deceleration of the body wave.

Fig. 5. Plot of lateral excursion of the apices of the median fins relative to the body for approximately one tail beat at $1.0\,L\,s^{-1}$. Values are means ± S.E.M. from four tail-beat cycles for all fish and are unfiltered. Note that sometimes the standard error is small enough to be contained by the data symbol. Black circles represent a point at $80\%\,L$, gray circles represent the apex of the dorsal fin, white circles represent the apex of the anal fin, and triangles and squares represent the tips of the dorsal and ventral lobes of the caudal fin, respectively (inset). The lateral excursions of dorsal and anal fin tips are slightly less than 180° out-of-phase with the body, but are similar to each other in magnitude and phase. The phasing of the caudal fin is shifted ahead of the body, resulting from approximately one wavelength being contained between the point at $80\%\,L$ and the caudal fin. The amplitudes of the anterior median fins are similar to the amplitude of the point 80% down the body.
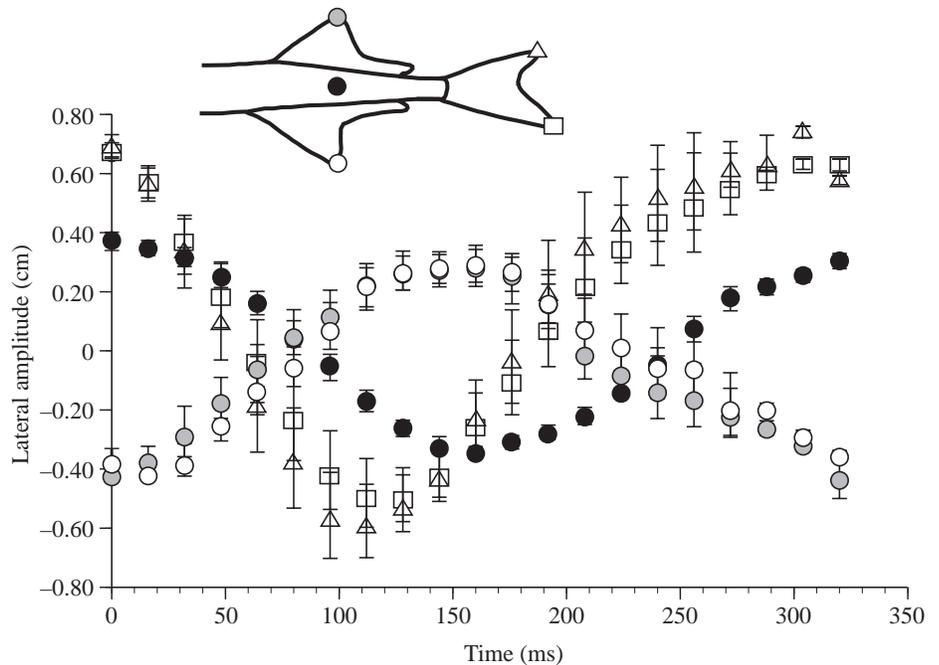
Discussion

Body kinematics of undulatory locomotion in needlefish

The term anguilliform locomotion can be ambiguous. At times it refers generally to the undulatory swimming motion of elongate animals, and at other times it refers specifically to the proportion of the body that undulates or to the number of sine waves present on the body at any given instant. While the definitions of some authors include whole-body undulation (Webb, 1975; Lindsey, 1978; Blake, 1983), Breder's original definition of anguilliform locomotion (Breder, 1926) does not specify the proportion of the body that undulates. It is clear that these authors use these broad classifications to refer to swimming at 'normal' or intermediate speeds. However, it is also clear that the proportion of the body that undulates changes with speed (Lighthill, 1969; Gillis, 1998). Breder's definition states that at least one half-wavelength and often more than one wavelength is present on the body at any time (Breder, 1926). According to this definition, needlefish are anguilliform swimmers, despite the fact that they do not undulate their entire body at low speeds, as has also been observed in eels (*Anguilla rostrata*) (Gillis, 1998). When needlefish undulate their entire body at higher speeds ($1.0\,L\,s^{-1}$ and above), they have approximately 1.5 waves along the length of their body, similar to anguilliform-swimming salamanders (*Siren intermedia*) (Gillis, 1997). Unlike salamanders, which maintain a constant propulsive wavelength ($64\%\,L$) across speeds, needlefish and eels increase their propulsive wavelength with speed (from 49 to $73\%\,L$ for needlefish and from 44 to $54\%\,L$ for eels).

Compared to eels (Gillis, 1998), needlefish exhibit substantially different body kinematics. For example, even when swimming at lower relative speeds, needlefish have a longer propulsive wavelength. If a longer propulsive wave is passed down the body at a constant speed similar to that in eels, then overall, needlefish would pass fewer waves down their body and therefore have a lower tail-beat frequency than eels. In contrast, the data show that at similar swimming speeds

them flush against the body surface (Fig. 8C). The insertion base of the pectoral fins in needlefish is positioned at approximately 35–40° relative to vertical.

Table 2. *Summary of* F-*tests for significance of effects in a three-way ANOVA with body-wave amplitude as the dependent variable*

Variable	Individual	Speed	Position	Individual× speed	Individual× position	Speed× position	Position×speed× individual
Body-wave amplitude	66.0*	101.92*	363.59*	37.0*	17.0*	59.43*	7.0*
(*L*)	(3, 252)	(2, 6)	(6, 18)	(6, 252)	(18, 252)	(12, 36)	(36, 252)

Data are from 4 individuals, 4 cycles per individual, 7 body points, at three swimming speeds.
Table entries are *F*-values, degrees of freedom are in parentheses.
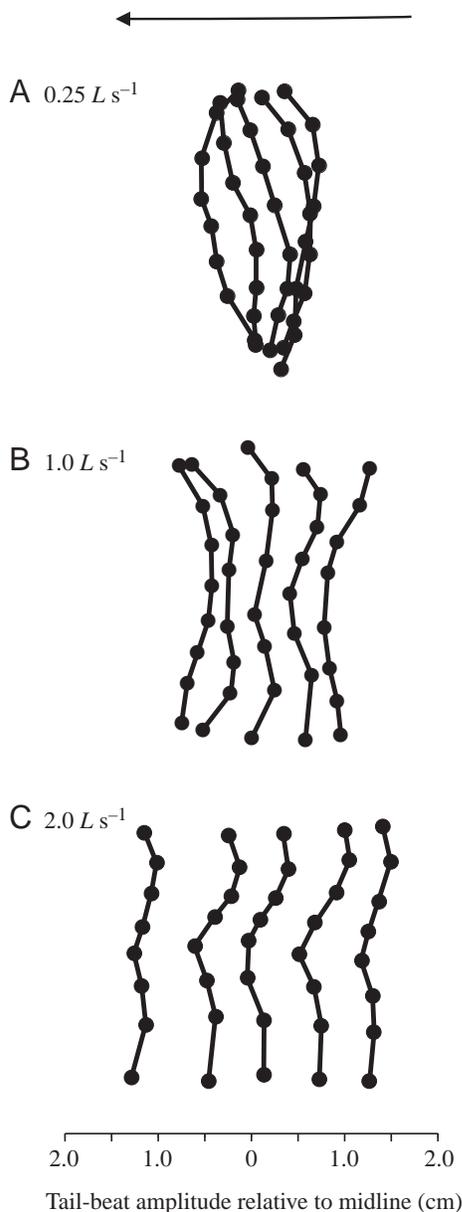*Significant at $P<0.001$.

Fig. 6. Posterior view of the digitized edge of the caudal fin as it beats from right to left (arrow) for one representative fish across three swimming speeds. The lateral displacement and configuration of the tail change dramatically as swimming speed increases. At the lowest speed, the dorsal lobe of the tail leads the ventral lobe. At higher speeds, the procurrent and middle rays of the caudal fin lead the tail as it sweeps to one side, causing the tail blade to adopt a 'W' conformation.

needlefish have higher tail-beat frequencies. Several reasons may explain this finding. The length of the propulsive wave may decrease as it passes down the body. Higher tail-beat frequencies may also be reflected by lower slip values, resulting in the need to pass more wavelengths down the body to swim at the same speed. In this respect, needlefish are less efficient anguilliform swimmers than eels. Finally, the needlefish studied here were approximately half the length of the eels studied by Gillis (1998). Despite comparisons at similar length-specific swimming speeds, this size difference may contribute to higher tail-beat frequencies in needlefish, since intraspecific size-dependent variation has been demonstrated in other fishes (Webb et al., 1984). Although needlefish have higher tail-beat frequencies than eels at any given swimming speed, the slope describing the increase in tail-beat frequency as a function of swimming speed is 39% lower in needlefish (Gillis, 1997).

Previous studies on swimming fishes have shown that while tail-beat frequency continues to increase linearly with swimming speed, tail-beat amplitude increases linearly only over a certain range of swimming speeds, after which it plateaus (Bainbridge, 1958; Webb, 1975; Blake, 1983). In needlefish, tail-beat amplitude does not plateau; it increases linearly over the range of swimming speeds investigated. This deviates from locomotor patterns of other fishes and may reflect the unique phylogenetic and ecological position of needlefish. Possessing an 'acceleration specialist' morphology does not seem to be the cause of this behavior, since esocids show a non-linear relationship between tail-beat amplitude and swimming speed (Webb, 1988). The maximum length-specific steady swimming speed for needlefish is relatively low compared to that of carangiform and labriform swimmers (Collette, 1977; Helfman et al., 1997). Thus, reports of high speeds attained by these piscivorous predators in the field probably reflect short, unsustainable bursts of acceleration. Alternatively, needlefish may be capable of swimming steadily at much higher speeds in the field.

In needlefish, the significant increase in stride length (Table 1) at high speeds is a consequence of relatively high slip values. A high slip value indicates a larger contribution to rearward, thrust-producing forces than lateral forces. In salamanders, slip values, and therefore stride lengths, decrease with increasing swimming speeds (Gillis, 1997), unlike eels which display a constant slip value and stride length across speeds (Gillis, 1998; D'Aout and Aerts, 1999). As typical of other swimmers, Froude efficiencies for needlefish increase with swimming speed. These values are higher than for tiger musky (*Esox* sp.), another fish with an 'acceleration specialist' body type (Webb, 1988). Although Froude efficiencies have not been reported for eels (Gillis, 1998; D'Aout and Aerts, 1999), their lower tail-beat frequencies would be likely to result in higher efficiencies compared to needlefish.

Gillis (1997) suggests that the maximum tail-beat amplitude of eels (8% L) is lower than that of sea snakes (*Pelamis platurus*) and salamanders (ranging from 11 to 19% L) due to the lateral compression of their body and to their continuous dorsal and anal fins (Graham and Lowell, 1987; Gillis, 1998). The increase in lateral surface area provided by fins facilitates a greater transfer of momentum from the fish to the water, suggesting that the median fins in needlefish can accelerate a relatively larger volume of water than the median fins of eels because of their position and size. It is not surprising, then, that needlefish exhibit lower tail-beat amplitudes and body wave amplitudes than eels at comparable swimming speeds (Gillis,

Fig. 7. Digitized outline traces of simultaneous posterior and ventral images of the pectoral fins during swimming at $0.25\,L\,s^{-1}$: thrust cycle and the beginning of the recovery cycle (from left to right). The body is drawn for reference and is not to scale. Hollow arrows indicate the direction of fin motion. (A) During the beginning of adduction, the dorsal edge of the fin is anterior to its ventral edge such that the plane of the fin is oriented obliquely relative to the transverse (z,y) plane. Rotation of the fin chord about its base causes the dorsal-most ray to move posteriorly relative to the ventral edge of the fin, which exposes a large surface area along the transverse plane. (B) At the end of adduction, the dorsal-most fin ray has completed rotation and has been retracted back towards the body wall, revealing its resting position above the dorsal surface of the body. (C) At the beginning of abduction, the dorsal-most ray leads the ventral-most ray in protraction, rotating the fin into the z,x plane so that it exposes the least surface area in the transverse plane to minimize drag. The time from the beginning of adduction to the end of adduction is 160 ms, while the time from the end of adduction to the beginning of abduction is 80 ms.
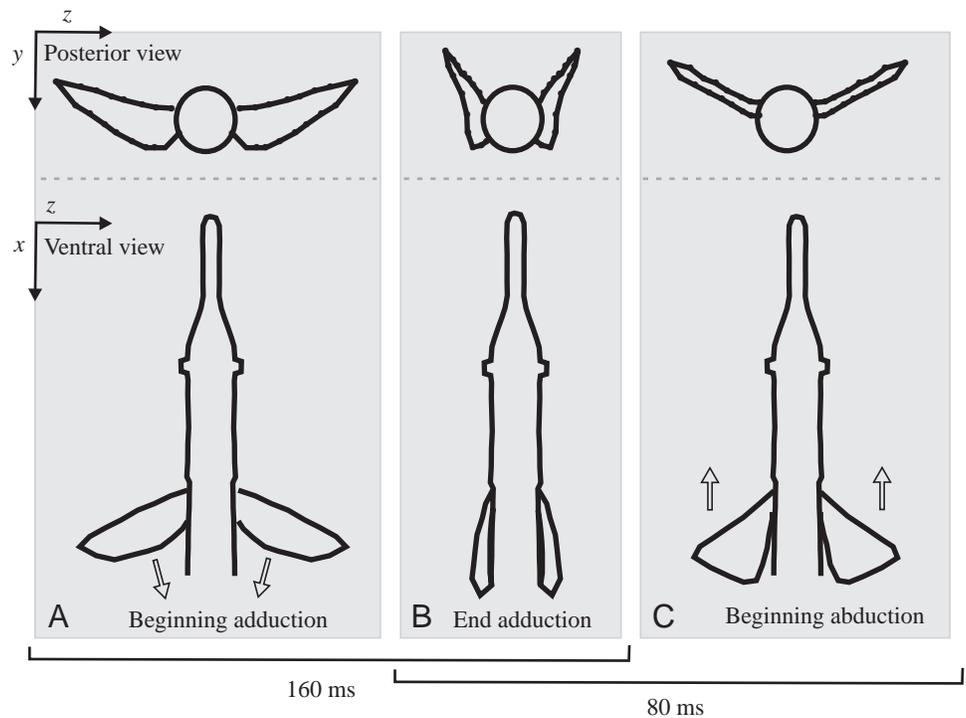
1998; D'Aout and Aerts, 1999). Similarly, Webb (1988) found that the posterior location of the dorsal and anal fins in musky correlated with relatively smaller tail-beat amplitudes and higher tail-beat frequencies when compared to rainbow trout (*Oncorhynchus mykiss*).

Decelerating propulsive wave

Steadily swimming fishes typically possess a propulsive wave that either maintains a constant speed or accelerates as it passes down the body, depending in part on the change in wave amplitude. Gillis (1997) found that eels and slow-swimming salamanders maintain a constant propulsive wave speed along the body, while sea snakes and fast-swimming salamanders possess an accelerating propulsive wave. The decelerating propulsive wave seen in fast-swimming needlefish is a novel finding for an anguilliform swimmer and is probably correlated with the size and location of the anterior median fins (Figs 1, 4C). Wavelength equals propulsive wave speed divided by tail-beat frequency, and since tail-beat frequency is fixed, by definition a decelerating propulsive wave must shorten in length. Gillis's (1998) observation that propulsive wave speed remains constant in eels is probably due to the uniform lateral profile created by their continuous median fins. At high swimming speeds the tapering posterior region of sirenid salamanders, which do not have fins to extend their lateral profile, causes the propulsive wave to accelerate. Not only is the speed of the posterior propulsive wave higher than in the front of the body, it is also higher than the posterior region of similarly sized eels as well (Gillis, 1997, 1998). Interestingly, although sea snakes increase the depth of their posterior body region with a fin-like keel and a flat, paddle-shaped tail, they also exhibit an accelerating propulsive wave (Graham and Lowell, 1987).

Function of the median fins

Discrete median fins can improve hydrodynamic efficiency and decrease drag in comparison to continuous median fins, especially when the gaps between fins are large (Lighthill, 1969; Webb, 1975). Theoretical and experimental work has shown that the wake shed by the dorsal and anal fins can be constructively utilized by the caudal fin (Weihs, 1973; Drucker and Lauder, 2001). Webb and Weihs have suggested a 'double-tail hypothesis', in which the propulsive body wave causes the dorsal and anal fins (the first 'tail') to be out of phase with the caudal fin, producing a relatively uniform thrust that is especially efficient for rapid acceleration (Weihs, 1973; Webb and Weihs, 1983). At $1.0\,L\,s^{-1}$, the caudal fin of the needlefish is indeed shifted out of phase with the anterior median fins, although not by 180°. Additional analyses show that dorsal and anal fin amplitudes remain relatively constant across swimming speeds, while body amplitudes increase. Initially, at the lowest speed the anterior median fins have a higher amplitude than the body, but at the highest swimming speed they both show similar magnitudes. In addition, as swimming speed increases, the tail-beat amplitude increases relative to the amplitude of the dorsal and anal fins. The apices of the dorsal and anal fins maintain a constant-phase relationship relative to the body across swimming speeds, suggesting that needlefish can modulate fin stiffness and height. Observations of needlefish suggest that at low speeds the dorsal and anal fins
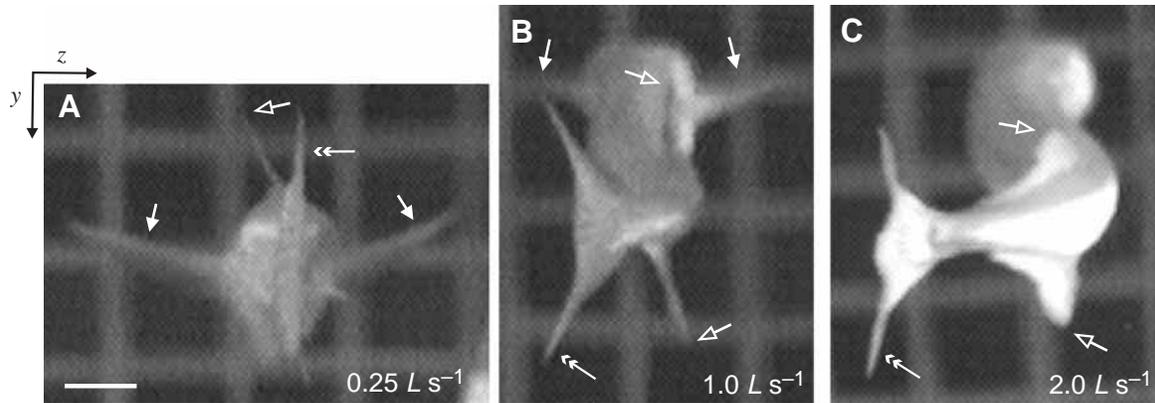
Fig. 8. Posterior view of one needlefish swimming steadily at three speeds, showing the position of the various fins. When the fins are not obstructed from view, arrows are used to denote their location. Solid arrows point to the pectoral fins, hollow arrows point to the tips of the dorsal and anal fins, and double-headed arrows point to the trailing edge of caudal fin. Scale bar, 1 cm. (A) At the lowest speed, the pectoral fins are clearly seen in the horizontal plane during mid-abduction. The dorsal fin is angled to the left of the body while the anal fin is obscured by the caudal fin, which is vertical and held in line with the body axis. (B) At intermediate speeds, the pectoral fins are held away from the body. The dorsal and anal fins are offset from the body midline, and the caudal fin adopts a W shape as it completes a beat to the left. (C) At the highest sustainable speed, the pectoral fins are held flush against the body and the W shape of the caudal fin becomes more exaggerated (see text for a description). From this view, the lateral excursion of the dorsal and anal fin is not clear, but as the tail beats to the left the flexible median fins lag towards the right of the fish. Note that the height of the median fins is not as great as in B.

move actively, yet currently there are no data to evaluate median fin wakes and their interactions with the caudal fin.

Conformation of the caudal fin

The caudal fin of a needlefish is a flexible structure that changes shape with swimming speed. At slow speeds, the dorsal lobe of the caudal fin leads the stiffer ventral lobe during each lateral excursion of a tail beat (Fig. 6), a kinematic pattern that has been noted for homocercal tails in other teleosts (Lauder, 2000). At higher swimming speeds, the procurrent and middle rays of the caudal fin lead the tail as it sweeps to one side. This causes the more flexible rays of the dorsal and ventral lobe to lag behind, creating a W shape (Figs 6, 8). This tail shape may serve to direct or accelerate flow into the wake behind the fish and is believed to facilitate thrust generation in scombrids such as Pacific bonito (*Sarda chiliensis*) and wavyback skipjack (*Euthynnus affinis*) (Fierstine and Walters, 1968).

Speed-dependent role of the pectoral fins

At the lowest swimming speed, needlefish oscillate their pectoral fins 31% faster than their tail-beat frequency. Outlines of simultaneous ventral and posterior views of a fish swimming at $0.25\,L\,s^{-1}$ (Fig. 7) indicate that the fin is feathered (tilted parallel to the frontal plane) during abduction and held to expose a large surface area along the transverse (y,z) plane during adduction. The speed of adduction is less variable and occurs faster than the speed of abduction. These lines of evidence typically suggest propulsive, drag-based locomotion (Gibb et al., 1994; Drucker and Jensen, 1997; Walker and Westneat, 1997). However, since the fin is brought back against the body at a slower speed than that which the water is moving past the body, no thrust can be produced (Webb and

Weihs, 1983). Why do needlefish oscillate their pectorals at high frequency, using a motion similar to drag-based propulsion, when they are not generating thrust with them? One possibility is that by continually oscillating their pectoral fins they may be able to react more quickly to generate forces over a range of directions. Using their pectoral fins may offer an additional degree of control over their forward swimming speed than if they were to swim with caudal fin propulsion alone. Observations in the field and in the laboratory support this idea; needlefish use their pectoral fins to decelerate body motions and facilitate directional changes of their prow-like cranium (Breder, 1926). Selective drag production anterior to the center of mass, rather than lift generation, may play an important role in stability control and adjustment of their force balance (Drucker and Lauder, 1999; Wilga and Lauder, 1999; Liao and Lauder, 2000).

At higher swimming speeds (up to $1.5\,L\,s^{-1}$), needlefish stop oscillating their pectoral fins and instead hold them abducted from the body (Figs 7C, 8B). Maintaining abduction of a pectoral fin with a vertically oriented base creates an acute angle described by the medial surface of the fin and the body, creating a positive dihedral that is often utilized in man-made aircraft to provide stability (Smith, 1992). Rolling about the long axis of the body was observed at low to intermediate swimming speeds but was not measured. By orienting their pectoral fins as a dihedral rather than parallel to the frontal (x,z) plane, needlefish may decrease roll and side-slip, a condition that is made worse by head yaw (Fig. 2) (Smith, 1992). There is evidence that other anguilliform swimmers also use their pectoral fins during steady locomotion. In Gillis (1998), fig. 1 shows the pectoral fins of *Anguilla rostrata* being held abducted while swimming steadily at $0.4\,L\,s^{-1}$. Unfortunately, whether the fin is oriented in the horizontal

plane or is held as a positive dihedral cannot be determined from the image.

Needlefish are the first fish in which a steady, positive dihedral conformation of the pectoral fins has been described (for a description of a negative dihedral, see Wilga and Lauder, 2000). Above $1.5\,L\,s^{-1}$, the pectoral fins of needlefish are completely folded against the body. These speed-dependent behaviors define two gait transitions, and distinguish them from most fishes, which only show one pectoral fin gait transition over their entire range of swimming speeds (Gibb et al., 1994; Jayne and Lauder, 1996; Drucker, 1996; Walker and Westneat, 1997).

References

Bainbridge, R. (1958). The speed of swimming of fish as related to size and to the frequency and amplitude of the tail beat. *J. Exp. Biol.* **35**, 109-133.

Blake, R. W. (1983). *Fish Locomotion*. Cambridge: Cambridge University Press.

Breder, C. M. (1926). The locomotion of fishes. *Zoologica* **4**, 159-297.

Collette, B. B. (1977). Belonidae. In: *FAO Species Identification Sheets for Fishery Purposes: Western Central Atlantic (Fishing Area 31)*, vol. 1 (ed. W. Fischer), p. 14. Rome: FAO.

D'Aout, K. and Aerts, P. (1999). A kinematic comparison of forward and backward swimming in the eel *Anguilla anguilla*. *J. Exp. Biol.* **202**, 1511-1521.

Drucker, E. G. (1996). The use of gait transition speed in comparative studies of fish locomotion. *Am. Zool.* **36**, 555-566.

Drucker, E. G. and Jensen, J. S. (1997). Kinematic and electromyographic analysis of steady pectoral fin swimming in surfperches. *J. Exp. Biol.* **200**, 1709-1723.

Drucker, E. G. and Lauder, G. V. (1999). Locomotor forces on a swimming fish: three-dimensional vortex wake dynamics quantified using digital particle image velocimetry. *J. Exp. Biol.* **202**, 2393-2412.

Drucker, E. G. and Lauder, G. V. (2001). Locomotor function of the dorsal fin in teleost fishes: an experimental analysis of wake forces in sunfish. *J. Exp. Biol.* **204**, 2943-2958.

Fierstine, H. L. and Walters, V. (1968). Studies in locomotion and anatomy of scombroid fishes. *Mem. S. Calif. Acad. Sci.* **6**, 1-31.

Gibb, A., Jayne, B. C. and Lauder, G. V. (1994). Kinematics of pectoral fin locomotion in the bluegill sunfish *Lepomis macrochirus*. *J. Exp. Biol.* **189**, 133-161.

Gillis, G. B. (1996). Undulatory locomotion in elongate aquatic vertebrates: anguilliform swimming since Sir James Gray. *Am. Zool.* **36**, 656-665.

Gillis, G. B. (1997). Anguilliform locomotion in an elongate salamander

(*Siren intermedia*): effects of speed on axial undulatory movements. *J. Exp. Biol.* **200**, 767-784.

Gillis, G. B. (1998). Environmental effects on undulatory locomotion in the American eel *Anguilla rostrata*: kinematics in water and on land. *J. Exp. Biol.* **201**, 949-961.

Graham, J. B. and Lowell, W. R. (1987). Surface and subsurface swimming of the sea snake *Pelamis platurus*. *J. Exp. Biol.* **127**, 27-44.

Gray, J. (1933). Studies in animal locomotion. I. The movement of fish with special reference to the eel. *J. Exp. Biol.* **10**, 88-104.

Helfman, G. S., Collette, B. B. and Facey, D. E. (1997). *The Diversity of Fishes*. Malden, MA: Blackwell Science.

Hove, J. R., O'Bryan, L. M., Gordon, M. S., Webb, P. W. and Weihs, D. (2001). Boxfishes (Teleostei: Ostraciidae) as a model system for fishes swimming with many fins: kinematics. *J. Exp. Biol.* **204**, 1459-1471.

Jayne, B. C. and Lauder, G. V. (1995). Speed effects on midline kinematics during steady undulatory swimming of largemouth bass, *Micropterus salmoides*. *J. Exp. Biol.* **198**, 585-602.

Jayne, B. C. and Lauder, G. V. (1996). New data on axial locomotion in fishes: how speed affects diversity of kinematics and motor patterns. *Am. Zool.* **36**, 642-655.

Jayne, B. C., Lozada, A. and Lauder, G. V. (1996). Function of the dorsal fin in bluegill sunfish: motor patterns during four locomotor behaviors. *J. Morph.* **228**, 307-326.

Lauder, G. V. (2000). Function of the caudal fin during locomotion in fishes: kinematics, flow visualization, and evolutionary patterns. *Am. Zool.* **40**, 101-122.

Liao, J. and Lauder, G. V. (2000). Function of the heterocercal tail in white sturgeon: flow visualization during steady swimmming and vertical maneuvering. *J. Exp. Biol.* **203**, 3585-3594.

Lighthill, J. (1975). *Mathematical Biofluiddynamics*. Philadelphia: Society for Industrial and Applied Mathematics.

Lighthill, M. J. (1969). Hydromechanics of aquatic animal propulsion: a survey. *Annu. Rev. Fluid Mech.* **1**, 413-446.

Lindsey, C. C. (1978). Form, function, and locomotory habits in fish. In *Fish Physiology*, Vol. VII, *Locomotion* (ed. W. S. Hoar and D. J. Randall), pp. 1-100. New York: Academic Press.

Nauen, J. C. and Lauder, G. V. (2000). Locomotion in scombrid fishes: morphology and kinematics of the finlets of the chub mackerel *Scomber japonicus*. *J. Exp. Biol.* **203**, 2247-2259.

Nelson, J. S. (1994). *Fishes of the World*. Third edition. New York: John Wiley & Sons.

Smith, H. C. (1992). *The Illustrated Guide to Aerodynamics*. Second edition. New York: TAB Books.

Walker, J. A. and Westneat, M. W. (1997). Labriform propulsion in fishes: kinematics of flapping aquatic flight in the bird wrasse *Gomphosus varius* (Labridae). *J. Exp. Biol.* **200**, 1549-1569.

Webb, P. W. (1975). Hydrodynamics and energetics of fish propulsion. *Bull. Fish. Res. Bd. Can.* **190**, 1-159.

Webb, P. W. (1988). 'Steady' swimming kinematics of tiger musky, an esociform accelerator, and rainbow trout, a generalist cruiser. *J. Exp. Biol.* **138**, 51-69.

Webb, P. W. and Keyes, R. S. (1981). Division of labor between median fins in swimming dolphin (Pisces: Coryphaenidae). *Copeia* **1981**, 901-904.

Webb, P. W., Kostecki, P. T. and Stevens, E. D. (1984). The effect of size and swimming speed on the locomotor kinematics of rainbow trout. *J. Exp. Biol.* **109**, 77-95.

Webb, P. W. and Weihs, D. (1983). *Fish Biomechanics*. New York: Praeger Publishers.

Weihs, D. (1973). The mechanism of rapid starting of slender fish. *Biorheology* **10**, 343-350.

Wilga, C. D. and Lauder, G. V. (1999). Locomotion in sturgeon: function of the pectoral fins. *J. Exp. Biol.* **202**, 2413-2432.

Wilga, C. D. and Lauder, G. V. (2000). Three-dimensional kinematics and wake structure of the pectoral fins during locomotion in leopard sharks *Triakis semifasciata*. *J. Exp. Biol.* **203**, 2261-2278.

Wolfgang, M. J., Anderson, J. M., Grosenbaugh, M. A., Yue, D. K. P. and Triantafyllou, M. S. (1999). Near-body flow dynamics in swimming fish. *J. Exp. Biol.* **202**, 2303-2327.

Zar, J. H. (1999). *Biostatistical Analysis*. Englewood Cliffs: Prentice-Hall, Inc.